



HAL
open science

Effect of pentagons in sp^3 systems on electronic, elastic, and vibrational properties: Case of chiral structures

Damien Connétable

► **To cite this version:**

Damien Connétable. Effect of pentagons in sp^3 systems on electronic, elastic, and vibrational properties: Case of chiral structures. *Physical Review B: Condensed Matter and Materials Physics* (1998-2015), 2011, vol. 83, pp. 035206 (1) -035206 (5). 10.1103/PhysRevB.83.035206 . hal-00842560

HAL Id: hal-00842560

<https://hal.science/hal-00842560>

Submitted on 8 Jul 2013

HAL is a multi-disciplinary open access archive for the deposit and dissemination of scientific research documents, whether they are published or not. The documents may come from teaching and research institutions in France or abroad, or from public or private research centers.

L'archive ouverte pluridisciplinaire **HAL**, est destinée au dépôt et à la diffusion de documents scientifiques de niveau recherche, publiés ou non, émanant des établissements d'enseignement et de recherche français ou étrangers, des laboratoires publics ou privés.



Open Archive Toulouse Archive Ouverte (OATAO)

OATAO is an open access repository that collects the work of Toulouse researchers and makes it freely available over the web where possible.

This is an author-deposited version published in: <http://oatao.univ-toulouse.fr/>
Eprints ID: 5543

To link to this article: DOI: 10.1103/PhysRevB.83.035206
URL: <http://dx.doi.org/10.1103/PhysRevB.83.035206>

To cite this version:

Connétable, Damien *Effect of pentagons in sp^3 systems on electronic, elastic, and vibrational properties: Case of chiral structures.* (2011)
Physical Review B (PRB), vol. 81 (n° 1). pp. 035206 (1) -035206 (5).
ISSN 1098-0121

Any correspondence concerning this service should be sent to the repository administrator: staff-oatao@listes.diff.inp-toulouse.fr

Effect of pentagons in sp^3 systems on electronic, elastic, and vibrational properties: Case of chiral structures

Damien Connétable*

CIRIMAT UMR 5085, CNRS-INP-UPS, Ecole Nationale d'Ingénieurs en Arts Chimiques et Technologiques (ENSIACET),
4 allée Émile Monso, BP 44362, F-31030 Toulouse Cedex 4, France

(Received 29 October 2010; published 20 January 2011)

We present first-principles calculations of carbon and silicon chiral framework structures (CFSs). In this system, proposed recently by Pickard and Needs [Phys. Rev. B **81**, 014106 (2010)], atoms form only pentagonal cycles. This configuration enables unambiguous analysis of the effects of pentagons on electronic, vibrational, and thermodynamic properties. The local density approximation electronic band gaps in CFSs were found to be equal to or greater than those of clathrates using the same formalism, as confirmed by *GW* calculations: 1.8 and 5.5 eV for Si and C-CFS, respectively. We show that, as in clathrates, an increasing electronic band gap is correlated with the contraction of the valence bands, resulting from the frustration of the p shells. The electron localized function and Wannier analysis confirm the sp^3 nature of the bonds. Finally, we discuss vibrational and related properties. We show that CFSs present singularities, in particular, that the higher frequencies are not located at the Γ point.

DOI: 10.1103/PhysRevB.83.035206

I. INTRODUCTION

During the last decades, numerous studies have reported the discovery and understanding of the properties of new allotropic carbon/silicon structures. The theoretical and technological interests in these types of systems takes its origin in high-thermoelectrical-power materials, hard materials, and materials with a large-band-gap. sp^2 and sp hybridized systems have been intensively studied and discussed, in particular, graphite, graphene, graphane, and cluster systems. Many works on nanotubes or exotic sp^2 allotropic phases illustrate this.¹

Studying cage-like systems has led to the discovery of large-gap materials, exceptional plasticity, and even high electron-phonon coupling.^{2,3} It has been suggested that pentagons and sp^3 shells are at the origin of many of the features of clathrates. These strong modifications are associated with electronic^{2,4,5} and vibrational⁶ properties. Among this research on different allotropic structures, Pickard and Needs⁷ recently proposed a new hypothetical allotropic three-dimensional (3D) network: a chiral framework structure (CFS) where all atoms are linked through sp^3 -type hybridization. Unlike diamond or clathrates, where the networks are mostly composed of hexagonal rings, the originality of these structure is that atoms forms only pentagons.

In this paper, we study the effects of pentagons on CFSs. Local density approximation (LDA) and *GW* calculations are presented to evaluate electronic band gaps accurately. The electron localized function (ELF) and Wannier functions are also presented and discussed, to clarify the nature of bonds. We conclude with a discussion on vibrational (phonons and Raman spectra) and related properties.

II. COMPUTATIONAL DETAILS

Our calculations were performed within the LDA⁸ of the density functional theory (DFT).⁹ We used the QUANTUM-ESPRESSO¹⁰ (*QE*) package. Some of the calculations (quasi-particle study, based on the so-called *GW* approximation) were

also achieved using the ABINIT¹¹ package. A pseudopotential approach is used,¹² with a plane-wave expansion of the wave functions. To calculate cohesive energies and elastic and electronic properties, 60- and 30-Ryd cutoff energies were imposed for C and Si, respectively, and the Brillouin zones are sampled by $15 \times 15 \times 15$ \mathbf{k} grids. The use of such increased cutoffs allowed us to check the good convergence of our calculations. Emphasis was also placed on the calculation of accuracy band gaps using the *GW* approximation.^{11,13} The Plasmon pole approximation with Hartree convergence was employed to calculate the *GW* corrections. Cutoffs of 7 and 12 Ha, and 1200 bands for Si and C, respectively, were used for the magnitude of the $|q + G|$ basis vectors considered to build the screening, the susceptibility, and the dielectric matrix. We finally computed the dynamic properties from density functional perturbative theory:¹⁴ $8 \times 8 \times 8$ \mathbf{k} meshes and 60- or 30-Ryd cutoff energies with $3 \times 3 \times 3$ \mathbf{q} meshes.

III. GROUND STATE PROPERTIES

The system has hexagonal symmetry ($P6_122$; space group no. 178).¹⁵ Atoms are localized in the $6b$ Wyckoff position ($x, 2x, 1/4$). The free parameter x is almost independent of the element ($x \simeq 0.232$). In this configuration, atoms form pentagonal rings.

In Table I, we report the optimized lattice parameters, the formation energies, the bulk modulus (computed either from a Murnaghan fit or from the linear response), and the LDA band gaps of diamond and CFSs. Like Pickard and Needs,⁷ we found that in CFSs, diamond, and clathrates, lengths and angles of bonds¹⁶ are very similar. CFS phases are slightly less dense than those of diamond ($\sim 8\%$) and display a compressibility that is close to that of the diamond phase. Their formation energies are slightly higher than those of diamond, but of the same order of magnitude as those of clathrates.

We calculate the elastic constants as the second derivatives of the internal energy with respect to the strain tensor.

TABLE I. Lattice parameters (a_o and c_o , in Å), volume per atom (in Å³/atom), bulk modulus (B_o , in GPa), formation energies (E_f , in meV/atom; the reference state is the diamond), and band gaps (Δ_g , in eV).

	a_o	c_o	V	B_o	E_f	Δ_g
C-diam	3.58 ^c (3.57 ^a)	–	5.7	460 (545) ^a	0	3.9 (5.48) ^a
C-CFS ^b	3.57	3.37	6.2	389	112	4.12
C-CFS ^c	3.55	3.32	6.0	428	141	4.03
C-CFS ^d	3.54	3.34	6.0	413	150	4.02
Si-diam	5.41 ^c (5.43 ^a)	–	19.8	97 (99) ^a	0	0.62 (1.17) ^a
Si-CFS ^b	5.47	5.11	22.1	–	53	1.46
Si-CFS ^c	5.38	5.03	21.0	90	66	1.31
Si-CFS ^d	5.33	5.15	21.1	87	72	1.19

^aExperimental, from Ref. 17.

^bTheoretical, from Ref. 7; PBE calculations.

^c*QE* simulations, Murnaghan fit.¹⁸

^dABINIT simulations, linear response calculations.¹⁹

The elastic constants are listed in Table II. To illustrate the anisotropy of the elastic constants as a function of the crystallography, we have drawn 3D representations of diamond and a CFS (Fig. 1). In the basal plane, we note a cylindrical symmetry; elasticity is slightly anisotropic (in comparison to



FIG. 1. (Color online) Three-dimensional representations of elastic constants of carbon (C) diamond, C-CFS, and Si-CFS.

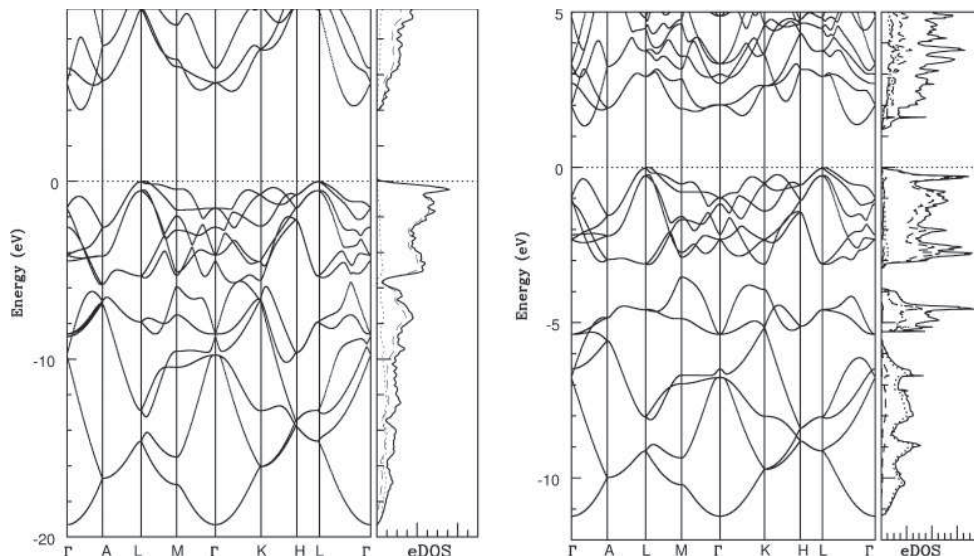


FIG. 2. *e*band and *e*DOS of carbon (left) and silicon (right) CFSs. Zero energy corresponds to the top of the valence bands. We have added the projected DOS on *s* and *p* shells (dotted and dashed lines, respectively).

TABLE II. Elastic constants (in GPa). $C_{66} = (C_{11} - C_{12})/2$.

	C_{11}	C_{33}	C_{44}	C_{66}	C_{12}	C_{13}	B_o
C-2	1092 ^a		585 ^a		135 ^a		458 ^a
	1076 ^b		576 ^b		125 ^b		560 ^b
C-CFS	972	893	523	386	198	155	428
Si-2	167 ^a		78 ^a		63 ^a		103 ^a
	166 ^b		79 ^b		64 ^b		98 ^b
Si-CFS	159	115	59	46	66	62	90

^aTheoretical LDA calculations, from Ref. 16.

^bExperimental, from Ref. 17.

metallic systems; see Ref. 20), while perpendicular to the basal plane (along the $\langle c \rangle$ axis).

IV. ELECTRONIC PROPERTIES

A. LDA electronic properties

We have plotted (Fig. 2) the electron density of states (DOS) and their band structures (*e*band) along high-symmetry directions. We notice, like Pickard and Needs,⁷ that the band gaps are indirect (between L and $\Gamma-A$). The most striking feature is the value of these band gaps. They are found to be equal to about 1.20 and 4.03 eV for silicon and carbon CFSs, respectively (the difference between ABINIT and *QE* calculations is due to the difference in lattice parameters). At this level of approximation, diamond's electron band gaps are found to be equal to 0.5 and 3.9 eV for Si and C, respectively. Gaps in CFSs are thus opened by 0.7 and 0.1 eV.

The analysis of the top of the valence bands shows that these states are essentially composed of *p* shells (see projected DOS on orbitals; Fig. 2). As in clathrates,⁵ *p* states in CFSs are also frustrated by pentagonal cycles. This frustration induces two main effects. First, a comparative analysis of the valence band width in CFS and in diamond reveals that the range

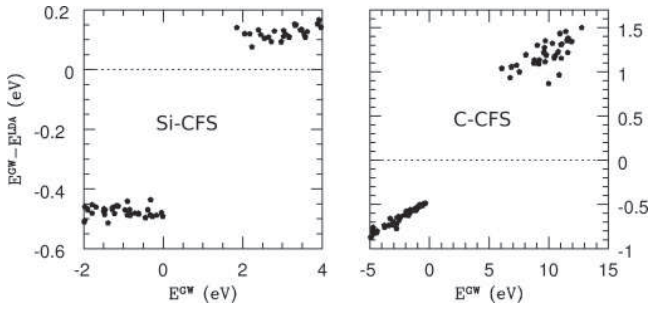


FIG. 3. Quasiparticle corrections $E^{\text{QP}} - E^{\text{LDA}}$ as a function of the quasiparticle energies E^{QP} for Si-CFS (left) and C-CFS (right).

of the C or Si bandwidth is strongly reduced (a reduction of about 3 and 1.5 eV for carbon and silicon, respectively) and that the main contraction is associated with the p shells. The second consequence is the high DOS at the top of the valence bands. As in the case of the Si-46 phase, we note that, in Si-CFS, a pseudogap opens within the valence bands.

B. GW CORRECTIONS

We then performed a quasiparticle energy calculation for both tetrahedral CFSs and compared them to those for diamond and clathrates. The corrections to the GW -Plasmon pole approximation are of the same order of magnitude as those found for tetrahedral analog systems:⁴ about 0.6 and 1.4 eV for Si and C, respectively (see Fig. 3). The correction for Si/C systems seems to be little dependent on the crystallography in sp^3 systems. The valence bands are “pushed” down, and conduction bands up. The electronic band gaps are also equal to 1.8 and 5.5 eV for Si and C CFS systems, respectively. Unlike carbon clathrates, the C-CFS gap is greater than that of diamond.

C. NATURE OF BONDS

To get a better understanding of the bonds, we have calculated the ELF²¹ for the carbon-CFS. According to its definition, the value of ELF is limited to the range of 0 to 1. A high value can be interpreted as a covalent interaction and a low ELF corresponds to an ionic interaction between unpaired electrons. From the calculated ELF displayed in Fig. 4 (see level curves), high values of contribution occur along C-C

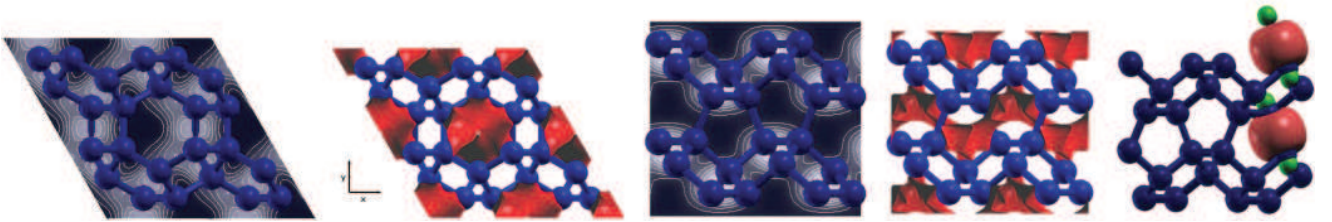


FIG. 4. (Color online) ELF topological analysis of carbon-CFS bonds: projection along the $\langle c \rangle$ axis (top) and the $\langle y \rangle$ axis (bottom). We plotted level lines (eight level steps: low and high ELF in black and in white, respectively) in the $[100]$ plan (left) and the isosurface of the small ELF contribution (right). The last figure represents one Wannier function along one bond: atoms are shown in dark blue. Red and green balls represent positive and negative contributions of Wannier functions.

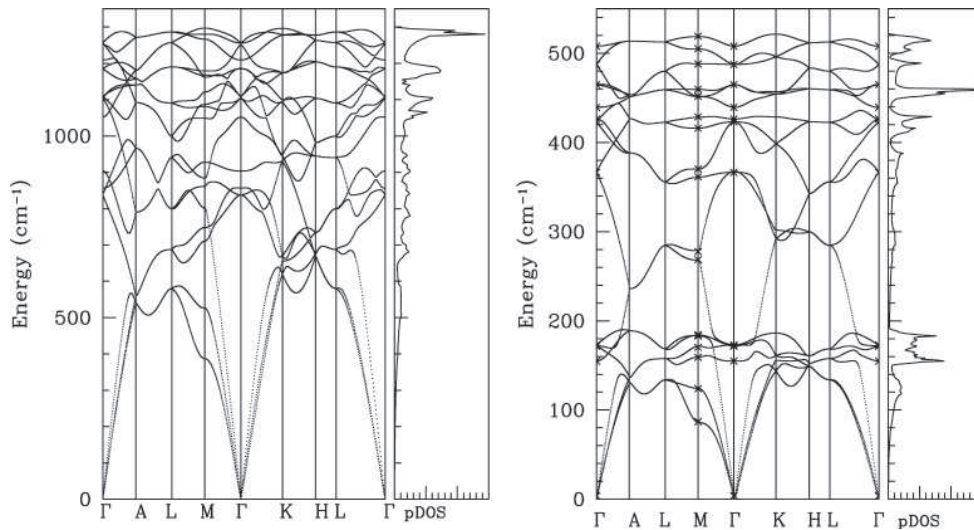


FIG. 5. Vibrational band structure and density of states (DOS) of carbon (left) and silicon (right) CFSs. Dots represent frequencies calculated with strong convergence criteria (see note 25).

TABLE III. Frequencies at Γ and corresponding irreducible representations. Ra, Raman active; IR, infrared.

C-CFS	0 $E_1 + A_2$	837 E_2^{Ra}	856 $B_{1,2}$	902 A_2^{IR}	1047 A_1^{Ra}	1100 $E_1^{\text{IR,Ra}}$	1104 E_2^{Ra}	1180 $E_1^{\text{IR,Ra}}$	1202 $B_{1,2}$	1247 $B_{1,2}$	1250 E_2^{Ra}
Si-CFS	0 $E_1 + A_2$	155 $B_{1,2}$	172 A_2^{IR}	173 E_2^{Ra}	367 $E_1^{\text{IR,Ra}}$	423 E_2^{Ra}	426 $B_{1,2}$	439 A_1^{Ra}	465 $E_1^{\text{IR,Ra}}$	487 E_2^{Ra}	508 $B_{1,2}$

bonds, which is ascribed to the strong hybridization of the carbon states; this is consistent with the e DOS analysis. We can also see that the low ELF contribution draws helicoidal channels (see isosurfaces). These channels should be ideal spaces for inserting elements.

Complementary to the ELF, we calculated Wannier functions²² associated with valence states. The results—presented in Fig. 4—are characteristic of sp^3 systems (see Ref. 3).

V. VIBRATIONAL PROPERTIES

Finally, we report vibrational properties. Phonon spectra of CFSs also show differences in comparison to those of diamond. Uppermost branches are (“red-”) shifted (see vibrational DOS and band structures; Fig. 5). The value of this shift is of the same order of magnitude as we find in clathrates.¹⁶ This decrease in frequencies in optical modes is to be related to the frustration of modes. In the case of carbon, acoustic modes completely vanish, and the maximum of the optical

branches is not located in Γ but in \mathbf{K} and \mathbf{M} . In Si, we also find that the uppermost frequencies are not in Γ . Although it is a known feature in carbon systems (diamond, clathrates, nanotubes),^{23,24} in silicon it is unusual and is characteristic of the crystallography.²⁵ The decrease is the result of an “overbending” of the highest optical frequencies and is associated with sufficiently large interatomic force constants between second-nearest neighbors.²⁶

Raman spectra have also been computed from first principles (see Fig. 6).²⁷ CFSs (space group 178; $P6_122$) have 18 modes in Γ , distributed as: $A_1 + 2A_2 + 2B_1 + B_2 + 3E_1 + 3E_2$. E_1 , E_2 , and A_1 could be Raman active. A_2 and E_1 are infrared active. In Table III, we report the frequencies and their irreducible representations.

From the vibrational DOS, thermodynamic properties (C_v , S_{vib} , and F_{vib}) were calculated within the harmonic approximation. The evolutions of these quantities with regard to the temperature (not represented here) are quantitatively the same as those obtained for diamond structures. Thus, the zero-point energies do not modify the relative stability of the phases: 61 and 60 meV/atom for Si-diamond and Si-CFS, respectively.

VI. CONCLUSION

In conclusion, we report a complete study of C- and Si-CFS properties. We show that these structures should display large electron band gaps, greater than those of diamond and clathrate analog structures. The quasiparticle band gaps are found to be equal to 1.8 and 5.6 eV for Si- and C-CFSs, respectively. Analysis of the electron states shows that opening of the electron band gaps is the consequence of the contraction of the valence bands by the frustration of p shells, as in clathrate structures. Moriguchi *et al.*,²⁸ who have studied silisils—“zeolite without oxygen”—have proposed many energetically favorable structures (in comparison to diamond). Such structures, which present numerous odd cycles, should present original electronic and vibrational properties. A consequence of the high DOS at the top of the valence bands would be, for C-CFSs, strong electron-phonon coupling. Vibrational properties are presented. We show that silicon should present an unusually low frequency of higher modes at Γ .

ACKNOWLEDGMENTS

Calculations were performed using HPC resources from GENCI-IDRIS (Grant No. 2009-92282) and the supercomputer facilities at *Calimp* CICT Toulouse, France (Grant No. 2010-p0749). D.C. acknowledges O. Thomas for the plot in Fig. 1.

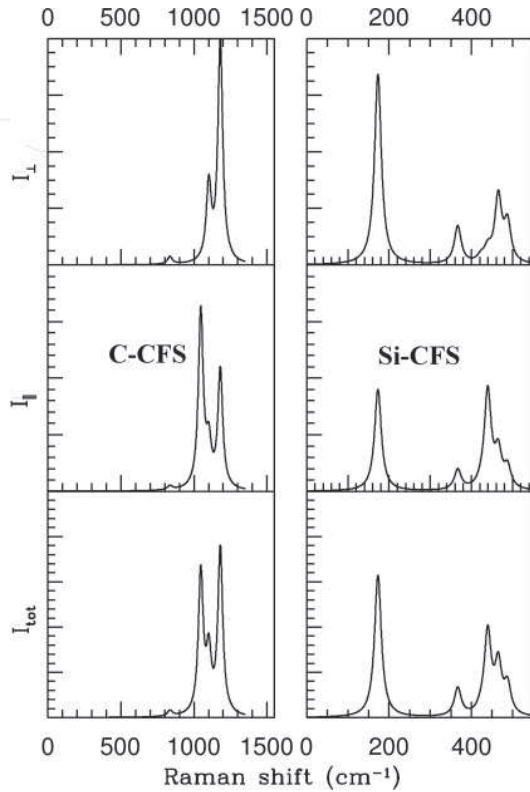


FIG. 6. Predicted Raman spectra of carbon (left) and silicon (right) CFSs. From top to bottom, perpendicular, parallel, and total intensities.

*Corresponding author: damien.connetable@ensiacet.fr

- ¹G.-M. Rignanese and J.-C. Charlier, *Phys. Rev. B* **78**, 125415 (2008).
- ²D. Connétable, V. Timoshevskii, E. Artacho, and X. Blase, *Phys. Rev. Lett.* **87**, 206405 (2001).
- ³X. Blase, E. Bustarret, C. Chapelier, T. Klein, and C. Marcenat, *Nature Mater.* **8**, 375 (2009).
- ⁴X. Blase, *Phys. Rev. B* **67**, 035211 (2003).
- ⁵P. Mélinon, P. Kéghélian, X. Blase, J. Le Brusq, A. Perez, E. Reny, C. Cros, and M. Pouchard, *Phys. Rev. B* **58**, 12590 (1998).
- ⁶D. Connétable, V. Timoshevskii, B. Masenelli, J. Beille, J. Marcus, B. Barbara, A. M. Saitta, G.-M. Rignanese, P. Mélinon, S. Yamanaka, and X. Blase, *Phys. Rev. Lett.* **91**, 247001 (2003).
- ⁷C. J. Pickard and R. J. Needs, *Phys. Rev. B* **81**, 014106 (2010).
- ⁸J. P. Perdew and A. Zunger, *Phys. Rev. B* **23**, 5048 (1981).
- ⁹P. Hohenberg and W. Kohn, *Phys. Rev.* **136**, B864 (1964); W. Kohn and L. J. Sham, *ibid.* **140**, A1133 (1965).
- ¹⁰P. Giannozzi, S. Baroni, N. Bonini, M. Calandra, R. Car, C. Cavazzoni, D. Ceresoli, G. L. Chiarotti, M. Cococcioni, I. Dabo, A. Dal Corso, S. Fabris, G. Fratesi, S. de Gironcoli, R. Gebauer, U. Gerstmann, C. Gougoussis, A. Kokalj, M. Lazzeri, L. Martin-Samos, N. Marzari, F. Mauri, R. Mazzarello, S. Paolini, A. Pasquarello, L. Paulatto, C. Sbraccia, S. Scandolo, G. Sclauzero, A. P. Seitsonen, A. Smogunov, P. Umari, and R. M. Wentzcovitch, *J. Phys. Condens. Matter* **21**, 395502 (2009).
- ¹¹X. Gonze, G.-M. Rignanese, M. Verstraete, J.-M. Beuken, Y. Pouillon, R. Caracas, F. Jollet, M. Torrent, G. Zerah, M. Mikami, Ph. Ghosez, M. Veithen, J.-Y. Raty, V. Olevano, F. Bruneval, L. Reining, R. Godby, G. Onida, and D. R. Hamann, and D. C. Allan, *Z. Kristallogr.* **220**, 558 (2005).
- ¹²N. Troullier and J. L. Martins, *Phys. Rev. B* **43**, 1993 (1991); N. Troullier and J. L. Martins, *Solid State Commun.* **74**, 613 (1990).
- ¹³F. Bruneval, N. Vast, and L. Reining, *Phys. Rev. B* **74**, 045102 (2006).
- ¹⁴S. Baroni, S. de Gironcoli, A. Dal Corso, and P. Giannozzi, *Rev. Mod. Phys.* **73**, 515 (2001).
- ¹⁵The properties of $P6_522$, the mirror structure of $P6_122$, are the same.
- ¹⁶D. Connétable, *Phys. Rev. B* **82**, 075209 (2010).
- ¹⁷C. Kittel, *Introduction to Solid State Physics* (Wiley, New York, 1996).
- ¹⁸F. D. Murnaghan, *Proc. Natl. Acad. Sci. USA* **30**, 244 (1944).
- ¹⁹D. R. Hamann, X. Wu, K. M. Rabe, and D. Vanderbilt, *Phys. Rev. B* **71**, 035117 (2005).
- ²⁰J.-M. Zhang, Y. Zhang, K.-W. Xu, and V. Ji Thin, *Solid Films* **515**, 7020 (2007).
- ²¹A. Savin, R. Nesper, S. Wengert, and T. Fässler, *Angew. Chem. Int. Ed. Engl.* **36**, 1809 (1997).
- ²²A. A. Mostofi, J. R. Yates, Y.-S. Lee, I. Souza, D. Vanderbilt, and N. Marzari, *Comput. Phys. Commun.* **178**, 685 (2008); N. Marzari and D. Vanderbilt, *Phys. Rev. B* **56**, 12847 (1997).
- ²³D. Connétable, G. M. Rignanese, J. C. Charlier, and X. Blase, *Phys. Rev. Lett.* **94**, 015503 (2005).
- ²⁴N. Mounet and N. Marzari, *Phys. Rev. B* **71**, 205214 (2005).
- ²⁵Frequencies at Γ and M points for Si-CFSs have been calculated, with higher convergence criteria (35 Ryd and a $15 \times 15 \times 15$ k grid). The results are reported in Fig. 5.
- ²⁶P. Pavone, K. Karch, O. Schütt, W. Windl, D. Strauch, P. Giannozzi, and S. Baroni, *Phys. Rev. B* **48**, 3156 (1993).
- ²⁷M. Lazzeri and F. Mauri, *Phys. Rev. Lett.* **90**, 036401 (2003).
- ²⁸K. Moriguchi, S. Munetoh, A. Shintani, and T. Motooka, *Phys. Rev. B* **64**, 195409 (2001).